Visual short-term memory for coherent and sequential motion: a rTMS investigation

Andrea Pavan[1,2*], Filippo Ghin[2,3], and Gianluca Campana[4,5]

[1]University of Bologna, Department of Psychology, Viale Berti Pichat, 5, 40127, Bologna, Italy

[2]University of Lincoln, School of Psychology, Brayford Wharf East, Lincoln LN5 7AY, United Kingdom

[3]Department of Child and Adolescent Psychiatry, Cognitive Neurophysiology, Faculty of Medicine of the TU Dresden, Fetscherstraße 74, 01307 Dresden, Germany

[4]Dipartimento di Psicologia Generale, University of Padova, Via Venezia 8, 35131, Padova, Italy.

[5]Human Inspired Technology Research Centre, University of Padova, Via Luzzati 4, 35121, Padova, Italy.

***Corresponding Author**

Andrea Pavan

University of Bologna

Department of Psychology

Viale Berti Pichat, 5, 40127

Bologna, Italy

E-mail: andrea.pavan2@unibo.it

 doi:10.20944/preprints202108.0569.v1

Abstract

We investigated the role of the human medio-temporal complex (hMT+) in the memory encoding and storage of a sequence of four coherently moving RDKs by applying repetitive transcranial magnetic stimulation (rTMS) during an early or late phase of the retention interval. Moreover, in a second experiment we also tested whether disrupting the functional integrity of hMT+ during the early phase impaired the precision of the encoded motion directions. Overall, results showed that both recognition accuracy and precision were worse in middle serial positions, suggesting the occurrence of primacy and recency effects. We found that rTMS delivered during the early (but not the late) phase of the retention interval was able to impair not only recognition of RDKs, but also the precision of the retained motion direction. However, such impairment occurred only for RDKs presented in middle positions along the presented sequence, where performance was already closer to chance level. Altogether these findings suggest an involvement of hMT+ in the memory encoding of visual motion direction. Given that both position sequence and rTMS modulated not only recognition but also precision of the stored information, these findings are in support of a model of visual short-term memory with a variable resolution of each stored item, consistent with the assigned amount of memory resources, and that such item-specific memory resolution is supported by the functional integrity of area hMT+.

Keywords: visual short-term memory, repetitive transcranial magnetic stimulation, visual memory precision, serial memory effects

 doi:10.20944/preprints202108.0569.v1

Introduction

Visual short-term memory (VSTM) is an active store of incoming visual information that is required for the completion of certain tasks and cognitive needs and allow to hold information for a few seconds [1]. The VSTM is closely connected to an individual's cognitive ability, can be investigated at the level of the neural circuits and is easily testable with specific procedures (see [2] for a review). VSTM involves the activity of many cortical areas such as frontal, occipital, posterior, and parietal cortices [3].

Behavioural research in humans showed that different attributes of visual stimuli are stored in visual short-term memory (VSTM). For example, McKeefry et al. [4] showed that stimulus characteristics such as orientation and direction of motion were stored in the VSTM. Pashler [5] and Vogel et al. [6] suggested that we can store up to 4 visual objects at one given time in the visual short-term memory, though Eng et al. [7] showed that the capacity of the VSTM was influenced by the perceptual complexity of the sample memory display. However, if there was a longer time frame for stimulus encoding, then more would be remembered. It was concluded that while complexity affects the capacity of the VSTM, it does not determine it.

Studies on human and non-human primates using a masking-delayed paradigm showed that VSTM for moving stimuli is maximally affected by the masking pattern when it is presented during the retention interval 0.2 s after the offset of the memory sample, and it has the same physical characteristics of the memory pattern (i.e., same motion direction, spatial location, and speed [8-10]. Further evidence has been also provided by brain imaging and brain stimulation studies, demonstrating that implicit VSTM for simple stimulus attributes relies on the same (low-level) cortical areas that process such attributes [11-13]. In the motion domain there is evidence that information about speed and direction can be accurately stored [14-16] and that the VSTM for such stimulus attributes is sensitive to early interference by an intervening masking stimulus. Pasternak and Zaksas [8] investigated the retention of motion in two macaque monkeys that were required to compare two sequentially presented coherent random dot kinematograms (RDKs) separated by a temporal delay [17-19]. The comparison/test stimulus was presented at a different location compared to that of the sample stimulus and a random-motion (noise) mask was introduced during the delay period in either the sample location or the location of the forthcoming comparison/test stimulus. The mask interfered with performance only when the mask was presented in the same location of the test, approximately 0.2 s after the start of the

 doi:10.20944/preprints202108.0569.v1

delay period, and when its speed matched that of the remembered sample. Therefore, the representation of coherent motion information in VSTM preserves direction, speed and spatial position and is most vulnerable to visual interference shortly after the completion of the sensory encoding phase [8,9]. This selectivity of masking effects resembles the selectivity shown in humans for spatial frequency, temporal frequency, and speed of gratings [4,15,20] suggesting that VSTM for these stimulus attributes might share similar mechanisms and neural substrates. Using a similar paradigm to that of Pasternak and Zaksas [8], Pavan et al. [10] showed that the visual mask mainly interfered with participants' performance when displayed 0.2 s after the offset of the sample and when it had a coherent direction rather than random directions. Moreover, the visual mask was significantly more effective when its direction and speed matched that of the remembered sample. These results support the notion that the memory representation of global motion is selective for direction and speed, being compromised by intervening directional stimuli presented immediately after the encoding phase.

In this study, we used repetitive transcranial magnetic stimulation (rTMS) to investigate the role of the human complex MT (hMT+), an area involved in visual motion processing [21,22], in both the serial encoding and storing of a sequence of coherently moving RDKs [23-25]. In two distinct experiments we aimed to interfere with the encoding and retention of sequential coherent motion information by delivering repetitive TMS (rTMS) over the left hMT+. In the first experiment participants had to memorize the direction of a motion sequence composed by four RDKs presented in rapid succession. The task was to report whether a probe RDK presented after the motion sequence and after a 3 s retention interval, was contained in the to-be-remembered motion sequence. In similar change detection tasks, in which participants were asked to detect the presence of suprathreshold changes among an array of items (including color, shape, motion direction, etc.) after a short retention period, results showed that observers were accurate for array sizes of up to 3 to 4 items or integrated objects defined as conjunctions of multiple features such as colors, orientations, shapes etc. [1,6,26,27]. In fact, based on these results, item-limit models of memory argue for a VSTM capacity of 3 - 4 independent memory slots, each storing information about an integrated visual object. In experiment 1, rTMS was delivered at 0.2 s (early rTMS) and 1.4 s (late rTMS) after the offset of the rapid motion sequence, respectively. The goal was to test whether rTMS delivered over the retention interval interfered with the encoding (for early TMS) and/or the retention (for late rTMS) of sequential

 doi:10.20944/preprints202108.0569.v1

coherent motion information. As previous studies found that the capacity of VSTM is up to four integrated visual objects [1,28], we expected early and late rTMS to interfere with the encoding and retention. Additionally, we also assessed the presence of serial effects (i.e., primacy/recency), and how rTMS affects motion sensitivity depending on the spatial position of the target in the sequence.

In the second experiment, we assessed whether rTMS interferes with the precision of the memory trace for motion direction and serial position in the temporal sequence. To this purpose we employed the same sequence of coherent RDKs and assessed the precision of the to-be-remembered direction of the motion stimulus in relation to their serial position in the temporal sequence. As mentioned above, previous studies have used change detection tasks in which participants were asked to spot changes in a display regarding different features of items such as the color, shape, orientation and were later asked to report the kind of change and the location where changes occurred [6]. Results from these studies contributed to the "*limited capacity memory model*". This model suggests that VSTM is saturated after 3 or 4 independent memory "slots" are filled, as participants only tended to be accurate in array sizes of up to 3-4 colors, shapes, orientations, or integrated objects which were described as a combination of these features [28]. Within this capacity model, each memory slot is responsible for holding information about an integrated visual item. Additionally, Kawasaki et al. [29] found that this capacity seemed to be even lower for motion direction as the average capacity limit was limited to about two slots. However, Bays and colleagues [30-33] argued that visual memory capacity is not fixed by the number of objects, as suggested by the limited capacity memory model, instead it is a resource which is also limited but it can be spread out and shared across all items available within the current visual scene. This implies that the precision of remembering an item is dependent on how much of the resource it demands, though memory precision is expected to decrease as the number of visual items increases. This approach led to the "*dynamic resource model of visual short-term memory*" which suggests that the resolution with which the visual object is stored in memory corresponds to the specific amount of memory resource assigned to that item [24,30-32,34,35]. Additionally, the same authors claimed that performance also depends on memory for object locations or serial position in a temporal sequence. In the second experiment we expect that rTMS delivered during the 3 s retention interval and 0.2 s after the offset of the motion sequence, mainly interferes with the precision of VSTM for motion direction

Preprints (www.preprints.org) | NOT PEER-REVIEWED | Posted: 31 August 2021 doi:10.20944/preprints202108.0569.v1

when the target RDK is presented at intermediate serial positions in the motion sequence (i.e., either 2 or 3).

Experiment 1

Methods

Participants

Two of the authors (AP and FG) and eleven naïve observers took part in this experiment. All participants had normal or corrected-to-normal visual acuity. Viewing was binocular. Each participant completed a questionnaire to assess for seizure, implanted metal objects, heart problems or any other psychiatric or neurological disease. Written informed consent was obtained from each participant. Methods were carried out in accordance with the World Declaration of Helsinki [36]. Data were collected at the University of Lincoln (UK) and the present study was approved by the local Ethics Committee of the University of Lincoln (protocol number: PSY1718170).

Apparatus

Stimuli were generated using Matlab Psychtoolbox [37-39] and displayed on a 20-inch HP p1230 monitor with a refresh rate of 85 Hz, with a screen resolution of 1280 x 1024 pixels. Each pixel subtended 0.032 deg (i.e.,~1.9 arc min). The mean luminance was 37.5 cd/m^2, with minimum and maximum luminance set to 0.08 cd/m^2 and 74.6 cd/m^2, respectively. A gamma-corrected lookup table was used so that luminance was a linear function of the digital representation of the image. Observers sat in a darkened room at 57 cm from the screen. The participant's head was stabilized by using a chin-head rest.

Stimuli

Stimuli were random dot kinematograms (RDKs) consisting of 200 white dots (dot diameter: 0.063 deg) presented within a circular aperture with a diameter of 9.4 deg (density: 2.85 dots/deg^2). All the dots moved along translational trajectories with 100% coherence. The dots moved on a grey background (mean luminance 37.5 cd/m^2) at a speed of approximately 5 deg/s [40]. The dots had a Weber contrast of 0.99. Dots had also a limited lifetime; that is, after 0.047 s each dot vanished and was replaced by a new dot at a different randomly selected

Preprints (www.preprints.org) | NOT PEER-REVIEWED | Posted: 31 August 2021 doi:10.20944/preprints202108.0569.v1

position within the circular window. Dots appeared and disappeared asynchronously on the display to avoid any flicker [41,42]. Limited lifetime and asynchronous dot displays were implemented to avoid attentional tracking of single moving elements. In addition, moving dots that travelled outside the circular window were replaced by a new dot at a different randomly location within the circular window, thus always maintaining the same dot density [40,43]. Dots could move towards one of eight directions (cardinal and intercardinal directions: 0°, 45°, 90°, 135°, 180°, 225°, 270°, 315°). For each motion sequence we randomly chose four directions with the constraint that they were always different (i.e., the minimum pairwise angular separation between directions was 45°).

Repetitive TMS

In order to localize the target cortical areas to stimulate and to set the TMS intensity, the phosphene threshold was estimated individually for each participant. rTMS stimulation was delivered through a MagPro X100 stimulator (Medtronic, Denmark) with a figure-eight coil of 90 mm. Participants wore a swimming cap. The target stimulation site was localized in all observers by using predetermined coordinates: 3 cm dorsal to inion and 5 cm leftward from there for the localization of hMT+. Our decision to stimulate the left hMT+ was due to previous evidence which showed, using TMS, a quite strong lateralization of motion perception in the left hemisphere [44,45]. Moreover, this localization technique has been used in previous studies [11,12,45-55] and provides a localization that is consistent with fMRI localizers [52,56]. In fact, in our previous rTMS study [52] we showed that hMT+ localization based on the craniometric procedure mostly overlaps with that based on neuro-navigation. In general, all the studies reported showed that TMS applied over hMT+ can produce moving or flickering phosphenes. Thus, the induction of moving or flickering phosphenes is considered a reliable method which can prevent confusing hMT+ with other adjacent cortical areas.

An adaptive procedure (i.e., rapid estimation of phosphene thresholds [REPT], [57]) was used to estimate the rTMS intensity for which participants perceived phosphenes in 60% of the trials with eyes closed and blindfolded. The adaptive staircase consisted of 30 trials. Phosphene thresholds were estimated delivering a cycle of 3 pulses in 100 ms (i.e., 30 Hz) over the left hMT+. On each trial, the participants had to verbally report whether they perceived phosphenes or not, and if they positively reported phosphenes, whether these were stationary or exhibited

Preprints (www.preprints.org) | NOT PEER-REVIEWED | Posted: 31 August 2021 doi:10.20944/preprints202108.0569.v1

some kind of moving or flickering patterns. For the stimulation over the left hMT+, the coil was always held tangential to the skull with the handle pointing upwards. The stimulation site was adjusted based on the characteristics of the phosphenes (e.g., moving, flickering, vivid, large), within 1 cm of radius from the point found with the craniometric procedure (i.e., 3 cm dorsal to inion and 5 cm leftward). Therefore, after the phosphene threshold phase, it is very likely that the stimulated area was hMT+ rather than other more posterior areas such as V3B/KO or LOC.

All our participants reported the perception of either moving or flickering phosphene patterns during stimulation of left hMT+. The mean rTMS intensity over hMT+ was 53.5% (SD: 6.39%) and 56.9% (SD: 6.47%) for experiments 1 and 2, respectively. An independent t-test revealed no significant difference between the stimulation intensities used in the two experiments (*Mann-Whitney U* = 67.5, $p = 0.268$). In a separate session, but on the same day, we also stimulated Cz as control site, to control for rTMS-related non-specific effects. The stimulation intensity over Cz was the same as for hMT+. At the beginning of each session, we estimated individually for each participant the phosphenes threshold delivering rTMS over hMT+, then the order of stimulation sites was randomized across participants. For the stimulation over Cz, the coil was always held tangential to the skull with the handle pointing backwards. This stimulation regime is the same as used in the main experiment (see the *Procedure* section).

Procedure

The procedure used in the experiment consisted of two phases: (i) *Training phase on motion direction discrimination*. Participants were trained in a motion-direction discrimination task to make sure that they were able to discriminate the direction of moving stimuli [40,43]. This phase of the experiment consisted of a single presentation interval (duration 0.15 s) in which an RDK was displayed at the center of the screen. The motion sequence of the RDK was the same as reported in the *Stimuli* section. Participants had to discriminate the motion direction of the coherent RDK, which could move in one of the eight cardinal and intercardinal directions (8AFC). Observers reported the motion direction of the coherent RDK using one of eight designated keys of the keypad of a standard UK computer keyboard. Each block consisted of 64 trials (with each direction presented 8 times), and participants performed as many blocks as needed to get an accuracy ≥ 0.95. (ii) *Main VSTM experiment*. The procedure used in the main experiment was similar to that used by Stäblein et al. [23]. Each trial begun with a fixation point

 doi:10.20944/preprints202108.0569.v1

presented for 1 s. The sample interval was composed of four RDKs (0.15 s each) presented in succession and with no blank interval between them. After the last RKD of the series, and after a retention interval of 3 s, another RDK was presented as test stimulus (Figure 1). The test RDK had the same properties of the RDKs presented in the sample (i.e., motion sequence). Participants were asked to memorize the direction of the four RDKs presented in the sample and report whether the direction of the test RDK was presented or not in the motion sequence (Yes/No task) by using the 'K' button to report '*present*' or the 'M' button to report '*absent*'. When the direction of the test RDK was present in the motion sequence, this could be the same as the RDK direction in any position of the sample motion sequence. For the sake of simplicity, we will refer to target RDK indicating the RDK in the sample motion sequence having the same direction to that of the test RDK. Participants had 3 s to respond after the presentation of the test RDK. In each rTMS session, the test RDK direction was included in the sample sequence in half of the trails, with equal probability of having the same direction either of the first, second, third or fourth RDK in the sample motion sequence. In the other half of the trials the test RDK had a different direction than those presented in the sample motion sequence.

For experiment 1, the temporal characteristics of the TMS stimulation was mainly based on the studies of [10,58]. In each session, rTMS (3 pulses every 100 ms – 1 pulse every ~33 ms; 30 Hz) was delivered either 0.2 s (*early* rTMS) or 1.4 s (*late* rTMS) after the offset of the sample motion sequence and during the 3 s retention interval. rTMS trials were interleaved by trials with no stimulation (i.e., No-TMS trials). Each combination of target serial position in the sample (i.e., first, second, third or fourth serial position), test RDK present or absent in the sample motion sequence, and TMS interval (i.e., No-TMS, *early* TMS, and *late* TMS) was presented six times. Therefore, each participant completed 144 trials (i.e., 4 target serial positions x 2 test RDKs [present/absent] x 3 TMS intervals x 6 repetitions) split into 8 blocks of 18 trials each. This was done to allow frequent breaks between blocks to avoid cumulative effects of rTMS and limit fatigue. Different conditions were randomly presented within each block. Within each session the stimulation site was kept the same. Before the main VSTM experiment participants were familiarized with the experimental procedure and completed a practice block of 24 trials (i.e., 4 target serial positions x 2 test RDK [present/absent] x 3 repetitions).

Preprints (www.preprints.org) | NOT PEER-REVIEWED | Posted: 31 August 2021 doi:10.20944/preprints202108.0569.v1

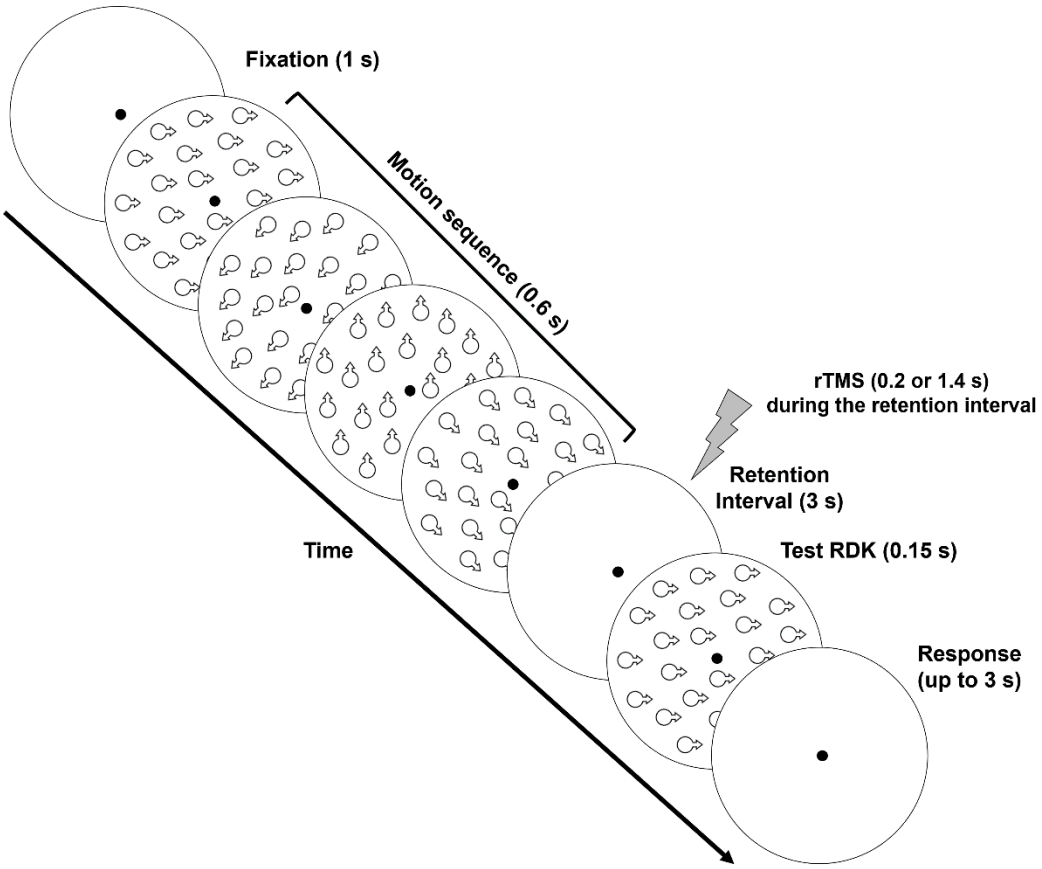

Figure 1. Schematic representation of stimuli and procedure used in the main rTMS VSTM experiment. An exemplary series of four RDKs moving in different directions is represented (sample motion sequence). After the 3 s retention interval, a test RDK is presented with the same direction as the first RDK in the sample motion sequence. rTMS (30 Hz) was delivered during the retention interval either 0.2 s or 1.4 s after the offset of the sample motion sequence. On each block, rTMS trials were randomly interleaved with No-TMS trials. Participants had 3 seconds to report whether the test RDK was presented or not in the sample motion sequence (Yes/No task).

Data Analysis

Individual Hit rates (*H*), i.e., when the participant correctly reported that the test RDK direction was present in the sample motion sequence, and individual False Alarm rates (*F*), i.e., when the participants erroneously reported that the test RDK direction was present in the sample motion sequence, were calculated as follows [58]:

Preprints (www.preprints.org) | NOT PEER-REVIEWED | Posted: 31 August 2021 doi:10.20944/preprints202108.0569.v1

$$H = \frac{\text{hits}}{\text{hits + misses}} \quad \text{Eq.1}$$

$$F = \frac{\text{False Alarms}}{\text{False Alarms + Correct Rejections}} \quad \text{Eq.2}$$

H and *F* rates were then converted in non-parametric measures of sensitivity and bias; called *A* and *b*, respectively. The *A* index is the corrected version of the *A'* index proposed by [59] and the *A"* index proposed by [60], and it was calculated with the correction introduced by [61]. We used a non-parametric measure of sensitivity to deal with the presence of some $H = 1$ (13.5% out of the total *hits* values calculated, i.e., 21/156; there were no $F = 0$) and the small number of responses per conditions (i.e., 6 repetitions per condition). *A* is a non-parametric estimate of the area under a proper Receiver Operating Characteristic (ROC) curve[1] (Pollack & Norman, 1964) that passes through any single point $p = (F, H)$ and that is less sensitive to extreme hit and false-alarm rates than the classic *d-prime* [62]. As pointed out in [61,63], based on standard Signal Detection Theory (SDT), *H* and *F* rates are transformed into indices of sensitivity (i.e., *d-prime*) and bias based on the assumption of normality of signal and noise distributions with equal variance. However, other transformations are possible including those not tied to an underlying statistical detection model, including ones based on the range of proper ROC curves that could pass through any single point. Additionally, these assumptions cannot be tested in Yes/No tasks, as rating tasks are required for this purpose (Stanislaw & Todorov, 1999). Therefore, we used *A* and *b* indexes as reported in [61]:

[1]Based on Zhang and Mueller [61], a proper ROC curve is a monotonically non-decreasing function with a non-increasing slope connecting the points (0,0) and (1,1) and necessarily lying above the line H = F. Therefore, a ROC curve between (0,0) and (1,1) is convex.

Preprints (www.preprints.org) | NOT PEER-REVIEWED | Posted: 31 August 2021 doi:10.20944/preprints202108.0569.v1

$$A=\begin{cases}\frac{3}{4}+\frac{H-F}{4}-F(1-\mathrm{H}) & \text{if } F\le 0.5\le H;\\ \frac{3}{4}+\frac{H-F}{4}-\frac{F}{4H} & \text{if } F\le H<0.5;\\ \frac{3}{4}+\frac{H-F}{4}-\frac{1-H}{4(1-\mathrm{F})} & \text{if } 0.5<F\le H;\end{cases} \quad \text{Eq.3}$$

$$b=\begin{cases}\frac{5-4H}{1+4F} & \text{if } F\le 0.5\le H;\\ \frac{H^2+H}{H^2+F} & \text{if } F<H<0.5;\\ \frac{(1-F)^2+(1-H)}{(1-F)^2+(1-F)} & \text{if } 0.5<F<H;\end{cases} \quad \text{Eq.4}$$

A sensitivity values ranges from 0 to 1.0, with 0.5 being considered the chance level and 1.0 perfect performance. Low values of *A* (i.e., below 0.5 and close to zero) could depend on sampling errors or response confusion [63]. *b* represents the slope of the proper ROC curve, and *b* values were *log* transformed to get a symmetric bias measure with respect to zero. The non-parametric bias measure *log*(*b*) ranges from -1.0 (extreme bias in favour of *yes* responses) to 1.0 (extreme bias in favour of *no* responses). A value of 0.0 means no response bias [63]. *A* and *log*(*b*) values were the input data for the statistical analyses. Data were analysed using R (R Core Team, 2019, v4.0.4; https://www.r-project.org/) in RStudio (RStudio Team, 2015, v1.4.1103; https://www.rstudio.com/).

Sensitivity/accuracy (*A* values) and bias (*log(b)*) values were analysed using generalized linear mixed effects models (GLMM) with '*lme4*' package [64]. For the analysis, we followed the protocol of [65,66] for data exploration, model selection and presentation. The Shapiro-Wilk test was used to test whether residuals were normally distributed. Outliers were identified using the median absolute deviation with a cut-off of 3 [67,68]. A Gamma function (experiment 1) or an Inverse Gaussian function (experiment 2) with an *identity* link transformation function were used in the GLMM. The *identity* link transformation function was used for *A* values (experiment 1) and precision values (experiment 2). An *identity* link function means that data were not

Preprints (www.preprints.org) | NOT PEER-REVIEWED | Posted: 31 August 2021 doi:10.20944/preprints202108.0569.v1

transformed. However, for the *b* values (bias) we used a *log* link transformation function, thus log-transforming *b* values. For experiment 1 we chose a Gamma function for the regression analysis because most of the *A* values fell into the Gamma quantiles, allowing to deal with the presence of outliers without removing them or transforming the original data. This is because the Gamma probability distribution allows greater variation for large mean values [65]. In general, Gamma and Inverse Gaussian distributions provided a better fit to the data because they can account for heteroscedastic patterns of increasing variability [69].

Results

Control Experiment for Direction Discrimination

The results of the control experiment for motion direction discrimination showed that participants, on average, needed 1.62 (SE: 0.33) training blocks to obtain the desired level of accuracy (≥ 0.95 correct performance rate). The mean accuracy at the control experiment for direction discrimination was 0.97 (SEM: 0.011). Given that the residuals were not normally distributed ($W = 0.78$, $p = 0.004$), a one-sided one-sample permutation tests (sampling permutation distribution 5k) showed that accuracies on the last training block were significantly higher than a median of 0.95 ($p = 0.0378$). Additionally, we tested whether the direction of the target had any effect on performance. The residuals were not normally distributed ($W = 0.44$, $p < 0.001$). A Friedman test on performance values of the last training block did not reveal a significant effect of the target direction ($\chi^2 = 5.82$, $df = 7$, $p = 0.56$). These results suggest that after the training blocks, participants' performance remains constant over cardinal and intercardinal directions of the target.

Main VSTM Experiment: sensitivity (A)

Figure 2 reports *A* values for each stimulation condition and target serial positions. Data from early and late rTMS were analysed separately to distinguish rTMS effects on the encoding and storing/retention phases of motion information.

Early rTMS

Figure 2a shows *A* values for early rTMS. A Shapiro-Wilk test showed that residuals were not normally distributed ($W = 0.97$, $p = 0.0013$) with a negative skewness of -0.554 (SE:

Preprints (www.preprints.org) | NOT PEER-REVIEWED | Posted: 31 August 2021 doi:10.20944/preprints202108.0569.v1

0.192). Seven outlier data points were identified (i.e., $A < 0.5$) and included in the analysis. A Gamma function and *identity* link transformation function were used in the GLMM model. In the analysis we included *A* values estimated in all the stimulation conditions, i.e., No-TMS, rTMS delivered over hMT+ and Cz. For the No-TMS trials, we calculated the average between the No-TMS trials in the hMT+ condition and those in the Cz condition. Additionally, we use the same No-TMS *A* values for the early and late rTMS conditions.

The selected model included as fixed factors the Stimulation Condition (i.e., No-TMS, rTMS over hMT+ and Cz), Target Position in the motion sequence and the interaction between Stimulation Condition and Target Position. Random effects of the selected model included random intercepts across participants and the participants' random slopes for the Stimulation Condition. The selected model reported a significant fixed effect of the Stimulation Condition ($\chi^2 = 6.24$, $df = 2$, $p = 0.044$), Target Position ($\chi^2 = 44.78$, $df = 3$, $p < 0.0001$) and a significant interaction between Stimulation Condition and Target Position ($\chi^2 = 18.63$, $df = 6$, $p = 0.0048$).

For the Stimulation Condition, pairwise post hoc comparisons corrected with False Discovery Rate (FDR; $\alpha = 0.05$) (Benjamini & Hochberg, 1995), did not reveal any significant difference between the three stimulation conditions (No-TMS, rTMS over hMT+ and Cz) (all *adjusted-p* > 0.05).

For the Target Position, pairwise post hoc with FDR correction, revealed a significant difference between position 1 and 3 (*adjusted-p* = 0.0026) and between position 3 and 4 (*adjusted-p* = 0.0006).

For the Stimulation Condition x Target RDK Position interaction, pairwise post hoc comparisons with FDR correction revealed a significant difference between target position 1 and 3 when rTMS was delivered over hMT+ (*adjusted-p* < 0.001), between target position 2 and 3 when rTMS was delivered over hMT+ (*adjusted-p* < 0.001), between target position 3 and 4 when rTMS was delivered over hMT+ (*adjusted-p* < 0.001), between rTMS over hMT+ and Cz for target position 3 (*adjusted-p* = 0.0005), and between No-TMS and hMT+ for target RDK in position 3 (*adjusted-p* = 0.0185) (for the interaction, the FDR correction was applied for 66 tests). Additionally, for target RDK position 3, there was not a significant difference between No-TMS and Cz conditions (*adjusted-p* = 0.764).

Overall, the results for early rTMS during the retention interval show low sensitivity values across all the conditions, suggesting that the task was quite difficult. Sensitivity was lower

Preprints (www.preprints.org) | NOT PEER-REVIEWED | Posted: 31 August 2021 doi:10.20944/preprints202108.0569.v1

when the target was presented in the second and third serial positions, suggesting the presence of serial effects in motion direction recalling (i.e., *primacy* and *recency* effects [70,71]. This was evident especially for the No-TMS condition for which a trend analysis reported a significant quadratic trend ($F_{1,12}$ = 10.81, p = 0.006) but not a linear trend ($F_{1,12}$ = 0.91, p = 0.36), and for the Cz condition, when averaging early and late rTMS data ($F_{1,12}$ = 7.83, p = 0.016). For the No-TMS condition, the minimum value of the quadratic function was A = 0.591, corresponding to a target serial position of 2.35, whereas for the Cz condition the minimum value of the quadratic function was A = 0.64, corresponding to a target serial position of 2.32. On the other hand, the quadratic trend was not evident for the hMT+ condition ($F_{1,12}$ = 2.07, p = 0.18). rTMS over hMT+ further reduced the sensitivity for the target when it was delivered 0.35 s after the offset of the third RDK in the motion sequence. This also suggests that rTMS maximally interfered with the encoding of the moving stimuli when delivered 0.35 s after the presentation of the moving RDK (Figure 2a).

A series of one-sided one-sample permutation tests (sampling permutation distribution 5k) were performed for each condition on A values to assess whether accuracy/sensitivity values across the stimulation conditions were greater than the chance level (0.5). The results showed that for the No-TMS condition all the A values were significantly greater than 0.5 ($p < 0.01$), but the A value estimated in position 3 (p = 0.0634). For the hMT+ condition we found the same results, with all the A values significantly higher than the chance level ($p < 0.05$) but the value estimated in position 3 (p = 0.41). For the Cz condition all the A values were significantly higher than 0.5 (all $p < 0.01$).

Preprints (www.preprints.org) | NOT PEER-REVIEWED | Posted: 31 August 2021 doi:10.20944/preprints202108.0569.v1

Late rTMS

For late rTMS (Figure 2b), A values were also analysed using GLMMs. A Shapiro-Wilk test showed that residuals were not normally distributed (W = 0.973, p = 0.0039) with a negative skewness of -0.565 (SE: 0.192). Seven outliers (low A values) were identified and included in the analysis. For A values estimated in the late rTMS condition the selected model included as fixed factors the Stimulation Condition (i.e., No-TMS, rTMS over hMT+ and Cz), Target Position and the interaction between Stimulation Condition and Target Position. Random effects of the selected model included random intercepts across subjects and the participants' random slopes for the Stimulation Condition. As for early rTMS, the model included a Gamma function and an identity link function. The model did report a significant effect of the Target Position (χ^2 = 20.43, df = 3, p = 0.00014), but not a significant effect of the Stimulation Condition (χ^2 = 1.25, df = 2, p = 0.54) or a Stimulation Condition x Target Position interaction (χ^2 = 6.29, df = 6, p = 0.39). For the Target Position, pairwise post hoc with FDR correction, revealed a significant difference between position 1 and 4 (*adjusted-p* = 0.011), position 2 and 4 (*adjusted-p* = 0.001) and position 3 and 4 (*adjusted-p* = 0.0001).

rTMS delivered approximately in the middle of the retention interval did not interfere with the storing/retention of the motion information. As for the early rTMS condition, we performed a series of one-sided one-sample permutation tests. For the hMT+ condition we found that all the *A* values were significantly higher than the chance level (p < 0.05), but the mean *A* value estimated in position 2 (p = 0.055). For the Cz condition all the *A* values were significantly higher than 0.5 (all p < 0.01).

Preprints (www.preprints.org) | NOT PEER-REVIEWED | Posted: 31 August 2021 doi:10.20944/preprints202108.0569.v1

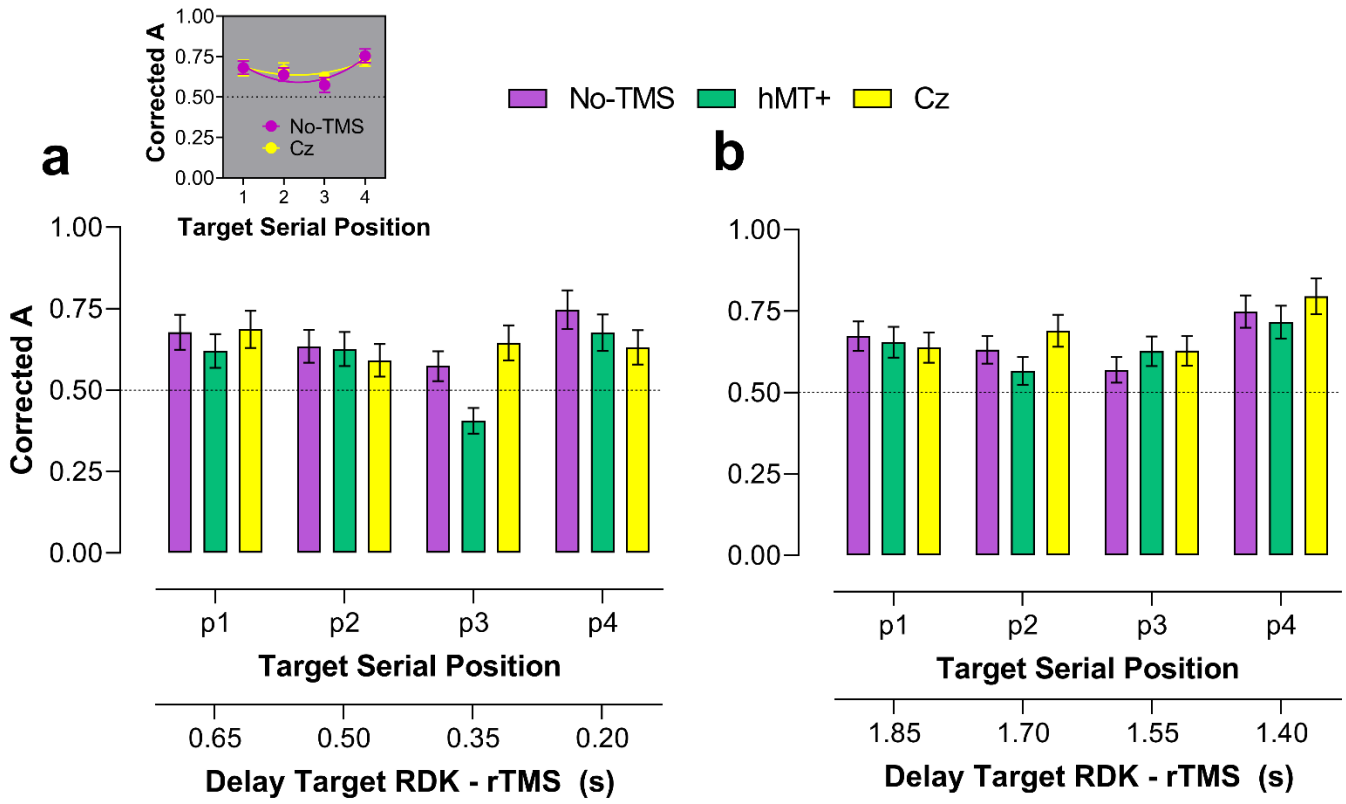

Figure 2. Mean *A* values for each serial position of the target RDK (1 to 4) and for each TMS condition (i.e., No-TMS, and rTMS over hMT+ and Cz). The plotted data and error bars were estimates from the output of the selected models for early and late rTMS. The horizontal dashed lines indicate the chance level (*A* = 0.5). The secondary x-axes indicate the time delay (in seconds) between the offset of the target RDK in the motion sequence and the onset of the rTMS. **(a)** Mean *A* values estimated for early rTMS (i.e., 0.2 s after the offset of the motion sequence). In this case, for target in position 1, rTMS was delivered after 0.65 s the offset of the first RDK. The insert above panel **(a)** shows the quadratic fit to the *A* values of the No-TMS and Cz conditions (averaged over the early and late rTMS conditions) of the form: $y = b0 + b1x + b2x^2$, where $b0, b1, b2$ are the coefficients of the polynomial function. No-TMS: $b0 = 0.90$, $b1 = -0.26$, $b2 = 0.06$, $R^2 = 0.8$, $SS = 0.003$; Cz: $b0 = 0.80$, $b1 = -0.14$, $b2 = 0.03$, $R^2 = 0.75$, $SS = 0.0014$. **(b)** Mean *A* values estimated for late rTMS (i.e., 1.4 s after the offset of the motion sequence). Error bars ±SEM.

Preprints (www.preprints.org) | NOT PEER-REVIEWED | Posted: 31 August 2021 doi:10.20944/preprints202108.0569.v1

Main VSTM Experiment: bias

Early rTMS

Figure 3 shows *log(b)* values for each stimulation condition and target position. As for sensitivity values, data from early and late rTMS were analysed separately. For early rTMS (Figure 3a), data were analysed using GLMMs. A Shapiro-Wilk test on non-transformed *b* values, showed that residuals were not normally distributed ($W = 0.978$, $p = 0.013$) with a positive skewness of 0.112 (SE: 0.192). Six outliers (positive and high *b* values) were identified and included in the analysis. In the analysis we included *b* values estimated in all the stimulation conditions, i.e., No-TMS, and rTMS delivered over hMT+ and Cz. As for *A* values, for No-TMS trials, we took the average between the No-TMS trials in the hMT+ condition and those in the Cz condition.

The selected model included as fixed factors the Stimulation Condition (i.e., No-TMS, rTMS over hMT+ and Cz), Target Position and the interaction between Stimulation Condition and Target Position. Random effects of the selected model included random intercepts across participants and the participants' random slopes for stimulation condition. The GLMM included a Gamma function and a *log* link function, so that *b* values were log-transformed. The model reported only a significant fixed effect of the Target Position ($\chi^2 = 15.16$, $df = 3$, $p = 0.0017$), but not of the Stimulation Condition ($\chi^2 = 5.17$, $df = 2$, $p = 0.076$), and Stimulation Condition x Target Position interaction ($\chi^2 = 3.5$, $df = 6$, $p = 0.74$).

FDR corrected post hoc comparisons for the Target Position reported a significant difference between positions 2 and 4 (*adjusted-p* = 0.034) and between positions 3 and 4 (*adjusted-p* = 0.001) (FDR was applied for 6 comparisons).

A series of two-sided one-sample permutation tests (sampling permutation distribution 5k) were performed for each condition on *log(b)* values to assess whether the bias measures were significant different from zero. The results showed that for the No-TMS condition all the log(b) values were not significantly different from zero ($p > 0.05$) but the *log(b)* value in position 4 ($p = 0.01$). For the hMT+ and Cz conditions all the *log(b)* values were not significantly different from zero ($p > 0.05$), indicating no response bias across the conditions.

Preprints (www.preprints.org) | NOT PEER-REVIEWED | Posted: 31 August 2021 doi:10.20944/preprints202108.0569.v1

Late rTMS

Figure 3b shows *log(b)* values for the late rTMS. A Shapiro-Wilk test on non-transformed *b* values, showed that residuals were not normally distributed ($W = 0.981$, $p = 0.03$) with a positive skewness of 0.516 (SE: 0.192). Four outliers (positive and high *b* values) were identified and included in the analysis. In the analysis we included *b* values estimated in all the stimulation conditions. The selected model included as fixed factors the Stimulation Condition (i.e., No-TMS, rTMS over hMT+ and Cz), Target Position and the interaction between Stimulation Condition and Target Position. Random effects of the selected model included only random intercepts across participants. The model included a Gamma function and a *log* link function. The selected model reported only a significant fixed effect of the Target Position ($\chi^2 = 22.5$, $df = 3$, $p < 0.0001$), but not of the Stimulation Condition ($\chi^2 = 2.04$, $df = 2$, $p = 0.36$), and Stimulation Condition x Target Position interaction ($\chi^2 = 3.89$, $df = 6$, $p = 0.69$). FDR corrected post hoc comparisons for the Target Position reported a significant difference between positions 1 and position 4 (*adjusted-p* = 0.014), between position 2 and position 4 (*adjusted-p* = 0.0009) and between positions 3 and 4 (*adjusted-p* < 0.0001).

A series of two-sided one-sample permutation tests (sampling permutation distribution 5k) were performed for each condition on *log(b)* values to assess whether the bias measures were significant different from zero. The results showed that for the hMT+ and Cz conditions, only the bias estimated for target RDKs in position 4 was significantly different from zero ($p = 0.038$ and $p < 0.0001$, for hMT+ and Cz respectively). For these two conditions the bias was negative thus indicating more '*yes/present*' responses.

Preprints (www.preprints.org) | NOT PEER-REVIEWED | Posted: 31 August 2021 doi:10.20944/preprints202108.0569.v1

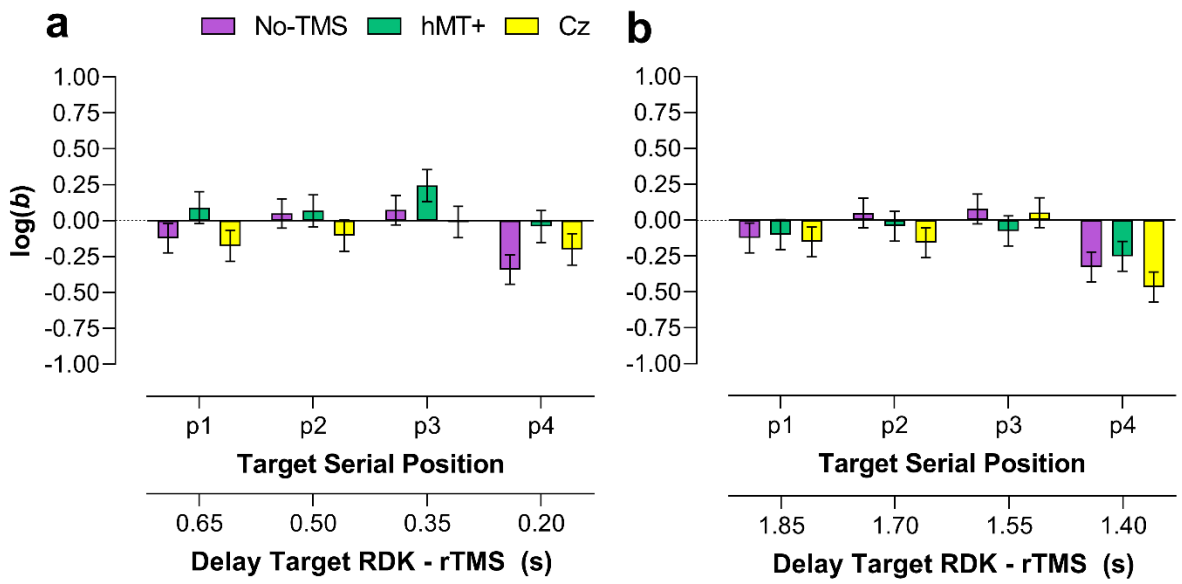

Figure 3. Mean bias [*log*(*b*)] for each serial position of the target RDK (1 to 4) and for each TMS condition. The plotted data and error bars were estimates from the output of the selected and fitted GLMM models for early and late rTMS. Data are symmetrical with respect to zero, with negative values indicating a bias towards *yes* responses, and positive values towards *no* responses. The secondary x-axes indicate the time delay (in seconds) between the offset of each RDK in the motion sequence and the onset of the TMS. **(a)** *log*(*b*) values estimated for early rTMS. **(b)** *log*(*b*) values estimated for late rTMS. Error bars ±SEM.

Discussion

The results of experiment 1 showed that when rTMS was delivered over the left hMT+ interfered with the encoding phase of the third target RDK in the motion sequence, that is when rTMS was delivered after 0.35 s from the offset of the target RDK. This effect is specific for the serial position in the motion sequence as there was not a significant difference between No-TMS and Cz for the same target serial position. However, the decrement in sensitivity/accuracy obtained after stimulating hMT+ was significantly lower than the accuracy values estimated in the No-TMS and Cz conditions. This effect is similar to that reported by van de Ven et al. [58], in which rTMS interfered with the encoding of the short-term representation of a complex shape when delivered 0.2 s after the stimulus presentation. The timing difference with respect to our experiment could depend on the different stimuli, timing and task used.

Preprints (www.preprints.org) | NOT PEER-REVIEWED | Posted: 31 August 2021 doi:10.20944/preprints202108.0569.v1

For the late TMS condition we found only an effect of the target position, but no effect of the TMS. In both early and late TMS conditions, the RDK in the last serial position (i.e., fourth position) had always higher sensitivity/accuracy than the other positions, suggesting a recency effect. Despite no main effect of rTMS and no interaction with target position, one-sided one-sample permutation tests found that rTMS over hMT+ produced *A* values that were not different from chance level only when the target was in the second serial position. This result suggests an effect of rTMS specific for intermediate target positions, similarly to what found in the early rTMS condition. Additionally, for the response bias we found only a significant effect of the target position, with less conservative responses (i.e., more '*yes/present*' responses) when the target was presented in the fourth serial position. However, no significant effects of the stimulation were found, suggesting that rTMS did not introduce any specific response bias.

Experiment 2

Methods

In the second experiment we assessed the effects of rTMS on the precision of VSTM for motion direction Importantly, we employed only the early rTMS condition, as in experiment 1 we found an effect of the stimulation only for the early condition. We used the same memory load as in experiment 1. Two of the authors (AP, FG) and six naïve participants took part to experiment 2. Apparatus, stimuli, and brain stimulation regime were the same as in experiments 1. However, in experiment 2 the RDKs could drift in a range of directions between 0 and 359.9 deg. To assign a specific motion direction to each RDK in the stimulus series, we originated an array of 3.6k directions ranging from 0 deg to 359.9 deg in steps of 0.1 deg. For each motion sequence we pseudo-randomly chose four directions with the constraints that the minimum pairwise angular separation between two consecutive directions was 45 deg, and that all the motion directions in the sequence were different.

The procedure used in experiment 2 consisted again of two phases: (i) an initial control experiment in which participants were trained in a motion-direction discrimination task to match their initial performance in terms of motion direction discrimination (Pavan et al., 2019; Pavan et al., 2016). This initial control experiment was the same as that used in experiment 1. (ii) Main VSTM precision experiment. The procedure used in the main experiment was similar to that used by Zokaei et al. [24] in their first experiment. The sample interval was composed of a series

Preprints (www.preprints.org) | NOT PEER-REVIEWED | Posted: 31 August 2021 doi:10.20944/preprints202108.0569.v1

of four RDKs with a duration of 0.5 s each. The duration of each RDK was longer than that used in the previous experiments as participants were asked to remember both the directions of the four patches and their position in the motion sequence.

The length of the stimulus series was always composed by four moving RDKs. After the last RKD of the series, and after a blank interval of 3.0 s, a probe was presented. The probe consisted of a frame circle of approximately the same diameter of the circular aperture of the RKDs, with a line of the same length of the radius starting from the center (Figure 4). At the top of the circular frame a digit indicated the target RDK in the stimulus series, the direction was to be reported (e.g., "2" = report the second RDK direction, "3" = report the third RDK direction, etc.). Participants were asked to adjust the orientation of the line inside the circular frame by using either the left or the right arrow, to match the direction of motion of the target RDK indicated by the digit appearing above the frame circle. The probe line was randomly positioned on a trial-by-trial basis around the circumference. The probability of probing any of the RDKs within the sequence was kept constant for all items in the series. The probe display was presented until participants had reported the direction of the target RDK and pressed the space bar to continue with the subsequent trial. Participants were instructed to respond as accurately as possible with no time pressure (reaction times were not recorded).

In total, there were 120 trials for each stimulation site (hMT+ and Cz). The total amount of trials was divided in 8 blocks of 15 trials each. Before the main VSTM precision experiment participants were familiarized with the experimental procedure and completed practice blocks of 12 trials each with no TMS in which the target serial position was randomized across trials (i.e., 3 trials per each spatial position). Participants performed up to three training blocks to familiarize with stimuli and task. The training blocks were also analyzed to assess whether participants performed the VSTM precision task above chance. During the main experiment, rTMS (30 Hz) was delivered on 50% of the trials 0.2 s after the onset of the three seconds retention interval.

Finally, errors between the target RDK direction and participants' responses were fitted with the variable precision (VP) model [35,72,73], to assess whether components of visual short-term memory differed across the three stimulation conditions (No-TMS, hMT+ and Cz).

Preprints (www.preprints.org) | NOT PEER-REVIEWED | Posted: 31 August 2021 doi:10.20944/preprints202108.0569.v1

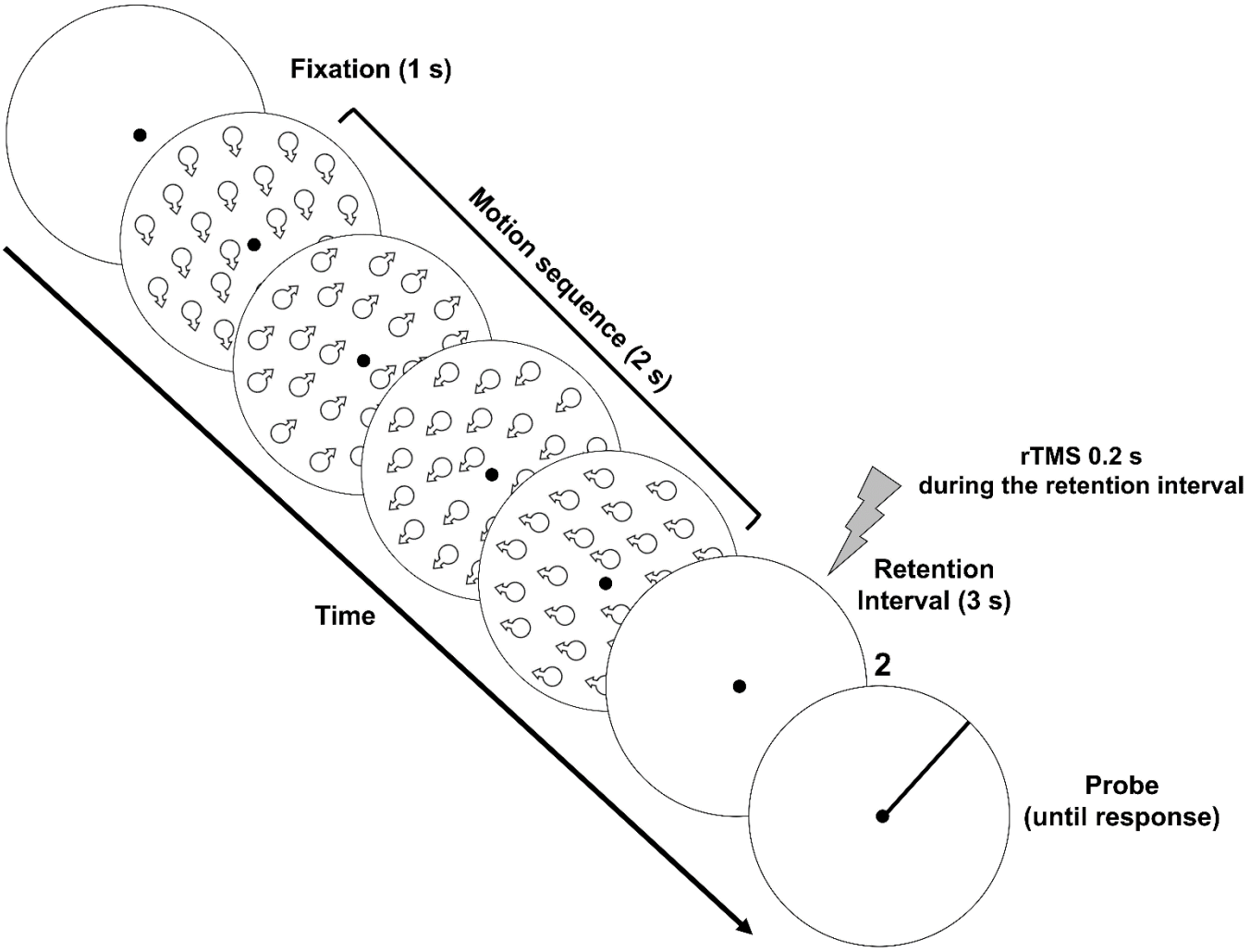

Figure 4. Schematic representation of stimuli and procedure used in experiment 2. An exemplary series of four moving RDKs is represented and the target to report is the second moving RDK in the series (indicated by the digit "2" above the probe stimulus). The small arrows in the motion sequence indicate given stimulus directions in a typical trial. For the sake of illustration, they depict motion direction in the figure, but were never presented during the actual experiment. The motion sequence was composed by a series of four RDKs presented for 0.5 s each (2 s in total).

Precision Calculation

Precision was defined as the inverse of the circular standard deviation of the angular distance (error in radians) between the target direction and the participant's response. Target and response directions (i.e., angles in radians) were wrapped to the interval [-π, π], such that odd,

Preprints (www.preprints.org) | NOT PEER-REVIEWED | Posted: 31 August 2021 doi:10.20944/preprints202108.0569.v1

positive multiples of π map to π and odd, negative multiples of π map to – π. The pairwise difference around the circle between target and response angles was then computed (i.e., error in radians) and finally we calculated the inverse of the circular standard deviation of the errors.

The mean circular standard deviation was calculated on 15 measures of error for each target position and stimulation condition. However, for the No-TMS trials the mean circular standard deviation was calculated on 30 measures of error, i.e., pooling the No-TMS trials for the hMT+ and Cz stimulation conditions. The angular distance (error) and circular standard deviation were calculated using the Matlab circular statistics toolbox (v1.21) [74,75]. Chance performance is expected to produce a precision value that approaches zero.

Results

Control Experiment for Direction Discrimination and Training blocks

The results of the control experiment for motion direction discrimination showed that the mean accuracy for direction discrimination was 0.98 (SEM: 0.008), with one training block for each participant. Given that the residuals were not normally distributed ($W = 0.80$, $p = 0.027$), a one-sided one-sample permutation tests (sampling permutation distribution 5k) showed that accuracies on the last training block were significantly higher than a median of 0.95 ($p = 0.0084$).

Participants, on average, performed 2.12 training blocks (SEM: 0.23). After the initial training, mean precision values across target spatial positions were: 3.65 (SEM: 0.67), 3.02 (SEM: 0.72), 3.05 (0.95), and 8.23 (SEM: 1.97) for target spatial position 1 - 4, respectively.

A series of one-sided one-sample permutation tests (sampling permutation distribution 5k) were performed for each target position on precision values to assess whether they were significantly above zero (i.e., chance level). The results showed that all the precision values across the four serial positions were significantly above chance (all $p < 0.005$).

Precision of VSTM for Motion Direction

Figure 5 shows VSTM precision as a function of the target serial position for each stimulation condition. As in the previous experiments, precision data were analysed using GLMMs. A Shapiro-Wilk test showed that residuals were not normally distributed ($W = 0.82$, $p < 0.001$) with a positive skewness of 1.456 (SE: 0.242). Eleven outliers were identified and

Preprints (www.preprints.org) | NOT PEER-REVIEWED | Posted: 31 August 2021 doi:10.20944/preprints202108.0569.v1

included in the analysis. The selected model included as fixed factors the Stimulation Condition (i.e., No-TMS, rTMS over hMT+ and Cz), Target Position in the motion sequence and the interaction between Stimulation Condition and Target Position. Random effects of the selected model included random intercepts across participants and the participants' random slopes for the target position. The model included an Inverse Gaussian distribution and an *identity* link function. The selected model reported a significant fixed effect of the Stimulation Condition (χ^2 = 11.5, *df* = 2, *p* = 0.0032), a significant effect of Target Position (χ^2 = 34.91, *df* = 3, *p* < 0.0001), and a significant interaction between Stimulation Condition and Target Position (χ^2 = 19.15, *df* = 6, *p* = 0.0039).

For the Stimulation Condition, pairwise post hoc comparisons with FDR correction, revealed a significant difference between Cz and No-TMS (*adjusted-p* = 0.025), between hMT+ and No-TMS (*adjusted-p* = 0.0032), but not between hMT+ and Cz (*adjusted-p* = 0.27).

For the Target Position, pairwise post hoc with FDR correction, revealed a significant difference between position 1 and 2 (*adjusted-p* = 0.0004), between position 1 and 3 (*adjusted-p* = 0.0032), between position 1 and 4 (*adjusted-p* = 0.0098), between position 2 and 4 (*adjusted-p* = 0.0001), between position 3 and 4 (*adjusted-p* = 0.004), but not between position 2 and 3 (*adjusted-p* = 0.24). This suggests the presence serial effects in remembering the target motion direction in the motion sequence, with positions 2 and 3 showing lower precision than positions 1 and 4. A trend analysis on precision values showed a significant linear ($F_{1,7}$ = 6.79, *p* = 0.035) and quadratic ($F_{1,7}$ = 13.16, *p* = 0.008) trend for the No-TMS condition, only a significant quadratic trend for the hMT+ condition ($F_{1,7}$ = 13.65, *p* = 0.008) (linear: $F_{1,7}$ = 0.97, *p* = 0.36), but any significant trend for the Cz condition (linear: $F_{1,7}$ = 4.95, *p* = 0.061; quadratic: $F_{1,7}$ = 4.87, *p* = 0.063).

For the Stimulation Condition x Target Position interaction, selected pairwise post hoc comparisons with FDR correction are showed in Table 1. The main result is that when the target RDK was in position 2 (i.e., when rTMS was delivered 1.2 s after the offset of the target patch in position 2), rTMS over hMT+ negatively affected the VSTM precision with respect to both Cz and No-TMS. Additionally, for this target position there was not a significant difference between Cz and No-TMS.

Preprints (www.preprints.org) | NOT PEER-REVIEWED | Posted: 31 August 2021 doi:10.20944/preprints202108.0569.v1

Stimulation Type		No-TMS				hMT+			
	Target Serial Position	p1	p2	p3	p4	p1	p2	p3	p4
hMT+	p1	0.894							
	p2		0.042*						
	p3			0.189					
	p4				0.015*				
Cz	p1	0.338				0.375			
	p2		0.288				0.0055*		
	p3			0.015*				0.204	
	p4				0.084				0.287

Table 1. Selected post hoc comparisons between precision values for the different stimulation types and for each target position. Significant *p* values are indicated with an asterisk.

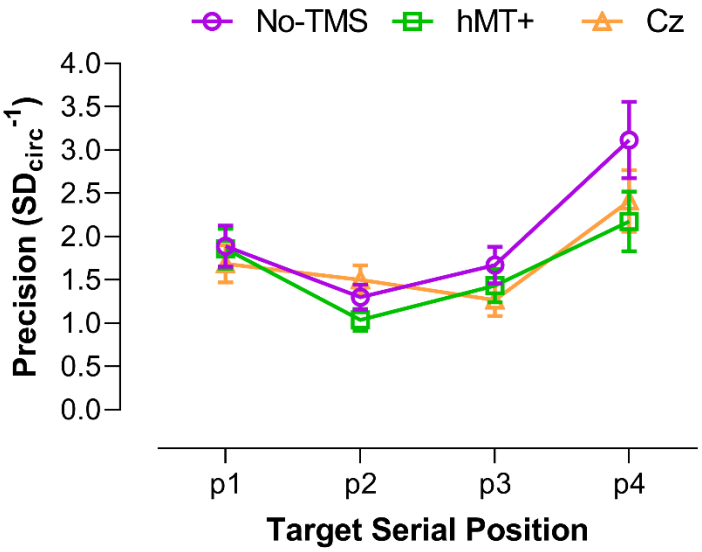

Figure 5. VSTM precision (calculated as the inverse of the circular standard deviation of the angular distance [error in radians] between the target direction and the participant's response) for each stimulation type (different curves) as a function of the target serial position in the motion sequence. Error bars ±SEM.

A series of one-sided one-sample permutation tests (sampling permutation distribution 5k) were performed for each condition to assess whether precision values across the stimulation

Preprints (www.preprints.org) | NOT PEER-REVIEWED | Posted: 31 August 2021 doi:10.20944/preprints202108.0569.v1

conditions and target positions were significantly higher than zero (i.e., chance level). The results showed that all the precision values were significantly higher than zero (all $p < 0.01$).

Modelling of Visual Short-term Memory

Delayed estimation tasks are particularly useful to assess the components of VSTM. In this account, in the VP model precision is variable across items and trials and previous studies have shown that visual short-term memory precision is indeed continuous and variable across memory items and trials [31,35,72,73]. In the VP model the amount of resource an item receives, thus regulating its encoding precision, varies randomly across memory items and trials and decreases with set size. The concept of resource may be linked to the gain (i.e., mean response amplitude) of a neural population pattern of activity encoding a memorized feature, such as colour, orientation, motion direction etc. The higher the gain, the higher the precision with which a stimulus is encoded [35]. The variability in gain across items and trials is consistent with single neuron firing rate variability [76] and the effects of attentional fluctuations in neural populations [77,78]. Therefore, following the rationale of Fougnie et al. [72], the VP model can be considered as an infinite scale mixture, a general framework that describes error distributions with a fixed mean and a precision (scale) that is sampled from some higher-order distribution, known as the 'mixing distribution'. In fact, in the model, precision is distributed according to some higher-order distribution, for example, a truncated normal or gamma distribution. When error is normally distributed around the correct value, and when precision (i.e., the inverse of variance) is gamma distributed, the resulting experimental data takes the form of a generalized Student's t-distribution wrapped on the circle, when considering stimulus dimensions such as colour, orientation, or motion direction. For guess rate (g), bias (μ), and SD (σ), the probability density function of this model is given by:

$$f(x;\ \mu, \sigma, g, v) = (g)\frac{1}{360} + (1 - g)\psi(x;\ \mu, \sigma, v) \qquad \text{Eq.5}$$

where ψ is the wrapped generalized Student's t-distribution and is:

Preprints (www.preprints.org) | NOT PEER-REVIEWED | Posted: 31 August 2021 doi:10.20944/preprints202108.0569.v1

$$\psi(x;\ \mu,\sigma,v) = \frac{c}{\sigma}\sum_{l=-\infty}^{\infty}\left(1+\frac{(x+360l-\mu)^2}{\sigma^2 v}\right)^{-(v+1)/2} \quad \text{Eq.6}$$

with

$$c = \Gamma\left(\frac{v+1}{2}\right) / \left(\Gamma\frac{v}{2}\sqrt{\pi v}\right) \quad \text{Eq.7}$$

(see [72] for more details on the VP model and mixing distribution).

The VP model we fitted to error values was characterized by three parameters: *guess rate* (*g*), the mean standard deviation of responses (*meanSD*), and the standard deviation of response error (*SDvar*). In this case, the standard deviations of observers' reports are assumed to be distributed as a normal distribution (Suchow et al., 2013). The *guess rate* (*g*) expresses the probability with which the observer does not remember the direction of the target patch probed in the test phase, and consequently guesses randomly. *MeanSD* represents the mean standard deviation of the precision of the remembered items, and it is inversely related to precision; high values in *meanSD* indicate a less precise memory representation. *SDvar* indicates intertrial variation in memory precision; high values of *SDvar* indicate high trial-to-trial variability.

The VP model was fitted to error values calculated using the circular distance (in radians) between the target RDK direction and the observer's response in the test phase. In our experiment we tested only one set size (i.e., four memory items on each trial). The VP model was fitted using the Matlab MemToolbox [79] (http://visionlab.github.io/MemToolbox/) to assess whether there were differences in *g*, *meanSD*, and *SDvar* between the three stimulation conditions. The model also included a bias term (μ) (using the function '*WithBias*' in MemToolbox), such that the central tendency of the data was not fixed at zero. However, only the parameters *g*, *meanSD*, and *SDvar* were analyzed.

The MemToolbox uses Bayesian inference to derive a probability distribution over parameter values. This probability distribution describes the reasonableness of parameters after considering the observed data considering a prior distribution (see [79] for a detailed description of model fitting and parameters estimation). The VP model was fitted to the entire set of each observer's data.

Preprints (www.preprints.org) | NOT PEER-REVIEWED | Posted: 31 August 2021 doi:10.20944/preprints202108.0569.v1

Results of the Variable Precision Model

Figure 6 shows the estimated parameters of the variable precision model. A Shapiro-Wilk test for normality revealed that residuals for *g* and *SDvar* were not normally distributed (*g*: $W = 0.9$, $p = 0.022$; *meanSD*: $W = 0.96$, $p = 0.52$; *SDvar*: $W = 0.52$, $p < 0.0001$) therefore the estimated parameters were analyzed using the aligned rank transform for non-parametric factorial analyses [80]. This analysis implements pre-processing steps that align not normally distributed data before applying averaged ranks after which ANOVA or a linear mixed model can be performed. This analysis was performed by using the statistical software *R* and the "*ARTtool*" package (http://depts.washington.edu/madlab/proj/art/). After the rank assignment, we performed a linear mixed model using the *lme4* package for R [81] with stimulation type as within-subjects factors, and with random intercept across subjects.

For *g* (Figure 6a), the non-parametric factorial analysis revealed a significant effect of the stimulation ($F_{2, 14} = 4.67$, $p = 0.028$). Post-hoc comparisons corrected for the False Discovery Rate (FDR; $\alpha = 0.05$) revealed only a significant difference between No-TMS and hMT+ ($p = 0.03$). For *meanSD* (Figure 6b) and *SDvar* (Figure 6c) the non-parametric factorial analysis did not report a significant effect of the stimulation type ($F_{2, 14} = 0.11$, $p = 0.89$; $F_{2, 14} = 0.195$, $p = 0.82$, for *meanSD* and *SDvar*, respectively).

In sum, fitting the errors data with the VP model (Fougnie et al., 2012) revealed that the three stimulation types do not differ in terms of the mean standard deviation of the precision of the remembered items (*meanSD*) or in terms of trial-to-trial precision variability (*SDvar*). However, rTMS over hMT+ significantly increased guess rate (*g*) with respect to the No-TMS condition, though the probability of guessing rate in the hMT+ condition was not significantly higher than the guess probability in the Cz condition.

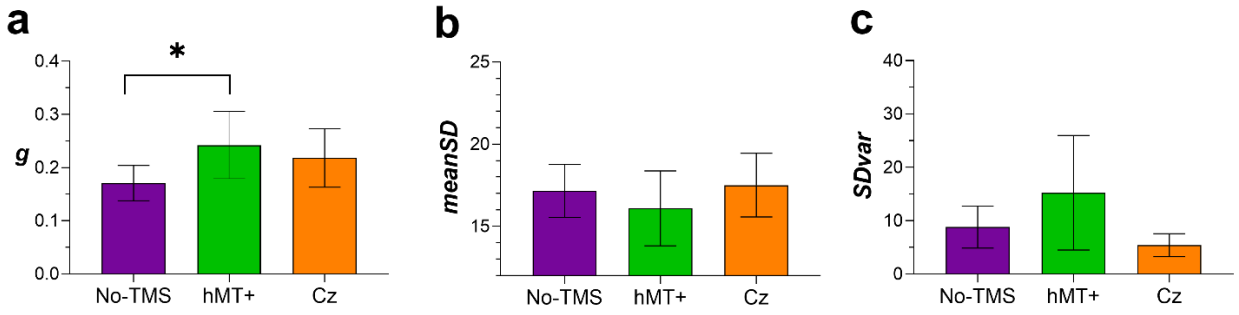

Preprints (www.preprints.org) | NOT PEER-REVIEWED | Posted: 31 August 2021 doi:10.20944/preprints202108.0569.v1

Figure 6. Mean parameters' estimates of the Variable Precision model. **(a)** *g* (random guessing) for No-TMS, hMT+ and Cz. **(b)** *MeanSD* (mean standard deviation of precision) for the three stimulation conditions. **(c)** *SDvar* (intertrial variation in memory precision). The asterisk represents the significant difference between No-TMS and hMT+ for *g*. Error bars ±SEM.

Discussion

The results of experiment 2 show that rTMS delivered over hMT+ 0.2 s after the motion sequence in the retention interval mainly interferes with the precision of the target patch in position 2, i.e., for the spatial position with a lower VSTM precision than positions 1 and 4. This clearly suggests the presence of serial effects, with positions 1 and 4 showing the highest VSTM precision (i.e., primacy and recency effects) and position 2 and 3 the lower precision, though there were no evident rTMS effects in position 3. A variable precision (VP) model fitted on response errors showed that these results may depend on a higher rate of random responses when rTMS was delivered over hMT+ with respect to the No-TMS condition, though the guess rate estimated in the Cz condition was approximately the same.

General Discussion

In two experiments, we investigated the neural underpinnings of VSTM for a sequence of moving stimuli by interfering with the encoding and retention of the memory trace by delivering rTMS over hMT+, a critical area for motion processing [42,82-87]. In the first experiment, we used a recognition task in which participants were asked to indicate whether a test RDK had the same motion direction of any of the four RDKs shown in the memory sample. Task performance was measured as sensitivity (*A*), a measure of accuracy, and an index of decisional bias (*log(b)*). rTMS was delivered either on the early (i.e., 0.2 s) or on the late part (1.4 s) of a 3 s retention interval. This procedure was designed to induce a stimulation-related interference either during the encoding phase or on the retention phase of the memory items, respectively. The results showed that when rTMS was delivered at the early stage of the retention interval over hMT+, the stimulation interfered with participants' sensitivity when the test RDK corresponded to the third RDK presented in the temporal sequence, thus when sensitivity was closer to the chance level. On the other hand, early TMS did not influence the bias measure.

 doi:10.20944/preprints202108.0569.v1

Furthermore, these results showed that early stimulation-related interference over the hMT+ in the retention interval might interfere with the encoding of the temporal sequence and the formation of the memory trace for motion directions. On the other hand, stimulation of the hMT+ later in the retention interval did not induce any significant modulation of sensitivity or bias. Therefore, we could argue that the lack of late TMS-induced interference during the retention interval suggests that hMT+ may not be directly involved in the retention process.

Importantly, these findings suggest that the visual complex hMT+ seems to be causally involved in the encoding of a sequence of visual moving stimuli in VSTM, whereas its role in retaining the motion sequence remains unclear. There is brain imaging evidence that multiple cortical sites may contribute to the retention and precision of visual information in VSTM. For example, the superior intraparietal sulcus (sIPS) may be involved in the modulation of the variability of visual working memory precision under increased memory load [88]. Additionally, a recent study of Zhao et al. [89] showed that the lateral occipital cortex (LOC) supports visual working memory precision, while the communication between the inferotemporal junction and LOC is modulated by the memory load, suggesting the presence of distinct neural mechanisms encoding for the memory load and precision variability.

In the second experiment, the precision of the encoded information was tested by asking participants to report the motion direction of one of the four RDKs presented in the memory sample with the adjustment method. The results showed that not only the functional integrity of hMT+ is causally involved in the strength of representation of items stored in VSTM, as measured with a sensitivity index, but it is also involved in encoding the precision of the memorized items. In fact, in experiment 2 we found a disruption of precision performance when rTMS was delivered over hMT+ and only for RDKs in the second temporal position.

Interestingly, previous studies have found that rTMS over the hMT+ showed different modulatory effects on the memory trace of stimuli presented in a temporal serial sequence. For example, Zokaei et al. [90] using a temporal sequence of two RDKs, found that rTMS over the hMT+ had opposite effects on memory precision depending on the position of the item in the temporal sequence. Specifically, in their study rTMS delivered either after the first or second RDK, decreased recall precision of motion direction only for the last item presented, but improved the recall precision of the first item in the motion sequence. The authors suggested that rTMS may have interfered only with the encoding of the last item that was in a privileged

 doi:10.20944/preprints202108.0569.v1

activation state by virtue of recency. It could be that the smaller recency effect boosted the recall precision of the first item in the temporal sequence. However, our results showed decreased VSTM precision only for RDKs presented in the middle of the temporal sequence (i.e., second and third positions), but no significant modulation for the last privileged item of the sequence. However, this might depend on differences between the experimental designs and stimulation protocols.

Furthermore, the results of the Variable Precision (VP) model showed that, when rTMS was delivered over the hMT+, the probability of random responses significantly increased with respect to the No-TMS condition, but not with respect to Cz. We did not find a significant difference between No-TMS and Cz and between hMT+ and Cz for the guessing rate. The other parameters of the VP model were not affected by the stimulation. Increased guessing responses can result from forgetting, lapses of attention, or encoding failures. Since early TMS pulses were presented at the end of the encoding phase in the retention interval (i.e., 0.2 s after the offset of the motion sequence) [8-10,58], it is possible that rTMS increased random guesses by interfering with the encoding of the four stimuli in the temporal sequence [91]. However, given that there was not a significant difference between hMT+ and Cz in terms of guess rate, it is possible that the results observed might depend on rTMS-induced distractibility, though there was not a significant difference between No-TMS and CZ, if this was the case. rTMS-induced increased of guessing rate probability has also been shown in previous findings. Redemaker et al. [91], showed that when participants had to remember the orientations of four briefly presented Gabor patches, recall errors were smaller when the visual field location targeted by rTMS overlapped with that of the cued memory item, compared to errors for stimuli probed diagonally to rTMS. Furthermore, early TMS pulses (i.e., immediately after the offset of stimulus presentation) impaired performance at all four locations, compared to late pulses (delivered in the middle of a 2 s retention interval). A mixture model [92] fitted to response errors showed that VSTM for orientation was more precise for items proximal to the pulse location, irrespective of pulse timing. However, guessing rate was higher with early TMS pulses than late pulses, regardless of stimulus location. The authors concluded that rTMS administered at the offset of the stimulus might disrupt early-phase consolidation of visual information. Taken together, these findings demonstrate the importance of the encoding phase mechanisms in early sensory cortices involved in the formation of short-term memory traces of visual information [58].

Overall, these findings provide further evidence that items in VSTM are not all-or-none representations; instead, such representations have different degrees of resolution, depending on the allocation of memory resources, on interference from other memory items, or from external factors such as perturbations induced by TMS. These types of representations are more compatible with a dynamic resource model of VSTM than with a limited capacity memory model [30-35]. In both experiments primacy and recency effects were evident, hence performance was better for the first and last RDK stimulus of the motion sequence, and worse for the stimuli presented in the middle of the temporal sequence. We speculate that this effect of serial position might be due, rather than to the intervention of long- and short-term memory mechanisms, to the interference of items with adjacent serial positions [93]. When the item is in the first position of the sequence, (backward) interference will come only from the successive item; similarly, when the item is in the last position of the sequence, (forward) interference will come only from the previous item. However, when the item is in a middle position, interference will come from both the previous and successive items in the sequence, thus producing larger interference. The presence of this serial dependence effect, not only in an all-or-none recognition task but also in a more subtle motion direction recall, suggests that each item in VSTM has a different degree of strength or activation, thus leading to a different precision judgement. This, in turn, is in support of a model of VSTM with a variable resolution of each stored item, consistent with the assigned amount of memory resources or serial effects.

Acknowledgments

This study was supported by the College Research Fund 2016/2017 of the University of Lincoln awarded to AP. We thank Holley Allen for help in data collection.

Author Contributions

Conceptualization A.P.; Methodology, A.P., F.G.; Software, A.P.; Validation, A.P., F.G.; Formal Analysis, A.P.; Investigation, A.P., F.G.; Resources, A.P.; Data Curation, A.P.; Writing – Original Draft Preparation, A.P., F.G., G.C.; Writing – Review & Editing, A.P., F.G., G.C.; Visualization, A.P.; Supervision, A.P., G.C.; Project Administration, A.P.; Funding Acquisition, A.P.

Conflicts of Interest

The authors declare no conflict of interest.

References

1. Luck, S.J.; Vogel, E.K. The capacity of visual working memory for features and conjunctions. *Nature* **1997**, *390*, 279-281, doi:10.1038/36846.
2. Luck, S.J.; Vogel, E.K. Visual working memory capacity: from psychophysics and neurobiology to individual differences. *Trends Cogn Sci* **2013**, *17*, 391-400, doi:10.1016/j.tics.2013.06.006.
3. van Lamsweerde, A.E.; Johnson, J.S. Assessing the Effect of Early Visual Cortex Transcranial Magnetic Stimulation on Working Memory Consolidation. *J Cogn Neurosci* **2017**, *29*, 1226-1238, doi:10.1162/jocn_a_01113.
4. McKeefry, D.J.; Burton, M.P.; Vakrou, C. Speed selectivity in visual short term memory for motion. *Vision Res* **2007**, *47*, 2418-2425, doi:10.1016/j.visres.2007.05.011.
5. Pashler, H. Familiarity and visual change detection. *Percept Psychophys* **1988**, *44*, 369-378, doi:10.3758/bf03210419.
6. Vogel, E.K.; Woodman, G.F.; Luck, S.J. Storage of features, conjunctions and objects in visual working memory. *J Exp Psychol Hum Percept Perform* **2001**, *27*, 92-114, doi:10.1037//0096-1523.27.1.92.
7. Eng, H.Y.; Chen, D.; Jiang, Y. Visual working memory for simple and complex visual stimuli. *Psychon Bull Rev* **2005**, *12*, 1127-1133, doi:10.3758/bf03206454.
8. Pasternak, T.; Zaksas, D. Stimulus specificity and temporal dynamics of working memory for visual motion. *J Neurophysiol* **2003**, *90*, 2757-2762, doi:10.1152/jn.00422.2003.
9. Pasternak, T.; Greenlee, M.W. Working memory in primate sensory systems. *Nat Rev Neurosci* **2005**, *6*, 97-107, doi:10.1038/nrn1603.
10. Pavan, A.; Langgartner, D.; Greenlee, M.W. Visual short-term memory for global motion revealed by directional and speed-tuned masking. *Neuropsychologia* **2013**, *51*, 809-817, doi:10.1016/j.neuropsychologia.2013.02.010.
11. Campana, G.; Cowey, A.; Walsh, V. Priming of motion direction and area V5/MT: a test of perceptual memory. *Cereb Cortex* **2002**, *12*, 663-669, doi:10.1093/cercor/12.6.663.
12. Campana, G.; Cowey, A.; Walsh, V. Visual area V5/MT remembers "what" but not "where". *Cereb Cortex* **2006**, *16*, 1766-1770, doi:10.1093/cercor/bhj111.
13. Sneve, M.H.; Alnaes, D.; Endestad, T.; Greenlee, M.W.; Magnussen, S. Modulation of activity in human visual area V1 during memory masking. *PLoS One* **2011**, *6*, e18651, doi:10.1371/journal.pone.0018651.
14. Blake, R.; Cepeda, N.J.; Hiris, E. Memory for visual motion. *J Exp Psychol Hum Percept Perform* **1997**, *23*, 353-369, doi:10.1037//0096-1523.23.2.353.
15. Magnussen, S.; Greenlee, M.W. Retention and disruption of motion information in visual short-term memory. *J Exp Psychol Learn Mem Cogn* **1992**, *18*, 151-156, doi:10.1037//0278-7393.18.1.151.
16. Magnussen, S.; Greenlee, M.W.; Thomas, J.P. Parallel processing in visual short-term memory. *J Exp Psychol Hum Percept Perform* **1996**, *22*, 202-212, doi:10.1037//0096-1523.22.1.202.

17. Bisley, J.W.; Pasternak, T. The multiple roles of visual cortical areas MT/MST in remembering the direction of visual motion. *Cereb Cortex* **2000**, *10*, 1053-1065, doi:10.1093/cercor/10.11.1053.
18. Bisley, J.W.; Zaksas, D.; Pasternak, T. Microstimulation of cortical area MT affects performance on a visual working memory task. *J Neurophysiol* **2001**, *85*, 187-196, doi:10.1152/jn.2001.85.1.187.
19. Zaksas, D.; Bisley, J.W.; Pasternak, T. Motion information is spatially localized in a visual working-memory task. *J Neurophysiol* **2001**, *86*, 912-921, doi:10.1152/jn.2001.86.2.912.
20. Magnussen, S.; Greenlee, M.W.; Asplund, R.; Dyrnes, S. Stimulus-specific mechanisms of visual short-term memory. *Vision Res* **1991**, *31*, 1213-1219, doi:10.1016/0042-6989(91)90046-8.
21. Amemiya, T.; Beck, B.; Walsh, V.; Gomi, H.; Haggard, P. Visual area V5/hMT+ contributes to perception of tactile motion direction: a TMS study. *Sci Rep* **2017**, *7*, 40937, doi:10.1038/srep40937.
22. Zeki, S. Area V5-a microcosm of the visual brain. *Front Integr Neurosci* **2015**, *9*, 21, doi:10.3389/fnint.2015.00021.
23. Stablein, M.; Sieprath, L.; Knochel, C.; Landertinger, A.; Schmied, C.; Ghinea, D.; Mayer, J.S.; Bittner, R.A.; Reif, A.; Oertel-Knochel, V. Impaired working memory for visual motion direction in schizophrenia: Absence of recency effects and association with psychopathology. *Neuropsychology* **2016**, *30*, 653-663, doi:10.1037/neu0000267.
24. Zokaei, N.; Gorgoraptis, N.; Bahrami, B.; Bays, P.M.; Husain, M. Precision of working memory for visual motion sequences and transparent motion surfaces. *J Vis* **2011**, *11*, doi:10.1167/11.14.2.
25. Zokaei, N.; Ning, S.; Manohar, S.; Feredoes, E.; Husain, M. Flexibility of representational states in working memory. *Front Hum Neurosci* **2014**, *8*, 853, doi:10.3389/fnhum.2014.00853.
26. Awh, E.; Vogel, E.K.; Oh, S.H. Interactions between attention and working memory. *Neuroscience* **2006**, *139*, 201-208, doi:10.1016/j.neuroscience.2005.08.023.
27. Wilken, P.; Ma, W.J. A detection theory account of change detection. *J Vis* **2004**, *4*, 1120-1135, doi:10.1167/4.12.11.
28. Luria, R.; Vogel, E.K. Shape and color conjunction stimuli are represented as bound objects in visual working memory. *Neuropsychologia* **2011**, *49*, 1632-1639, doi:10.1016/j.neuropsychologia.2010.11.031.
29. Kawasaki, M.; Watanabe, M.; Okuda, J.; Sakagami, M.; Aihara, K. Human posterior parietal cortex maintains color, shape and motion in visual short-term memory. *Brain Res* **2008**, *1213*, 91-97, doi:10.1016/j.brainres.2008.03.037.
30. Bays, P.M.; Husain, M. Dynamic shifts of limited working memory resources in human vision. *Science* **2008**, *321*, 851-854, doi:10.1126/science.1158023.
31. Bays, P.M.; Catalao, R.F.; Husain, M. The precision of visual working memory is set by allocation of a shared resource. *J Vis* **2009**, *9*, 7 1-11, doi:10.1167/9.10.7.
32. Bays, P.M.; Gorgoraptis, N.; Wee, N.; Marshall, L.; Husain, M. Temporal dynamics of encoding, storage, and reallocation of visual working memory. *J Vis* **2011**, *11*, doi:10.1167/11.10.6.

33. Bays, P.M.; Wu, E.Y.; Husain, M. Storage and binding of object features in visual working memory. *Neuropsychologia* **2011**, *49*, 1622-1631, doi:10.1016/j.neuropsychologia.2010.12.023.
34. Gorgoraptis, N.; Catalao, R.F.; Bays, P.M.; Husain, M. Dynamic updating of working memory resources for visual objects. *J Neurosci* **2011**, *31*, 8502-8511, doi:10.1523/JNEUROSCI.0208-11.2011.
35. van den Berg, R.; Shin, H.; Chou, W.C.; George, R.; Ma, W.J. Variability in encoding precision accounts for visual short-term memory limitations. *Proc Natl Acad Sci U S A* **2012**, *109*, 8780-8785, doi:10.1073/pnas.1117465109.
36. World Medical, A. World Medical Association Declaration of Helsinki: ethical principles for medical research involving human subjects. *JAMA* **2013**, *310*, 2191-2194, doi:10.1001/jama.2013.281053.
37. Brainard, D.H. The Psychophysics Toolbox. *Spat Vis* **1997**, *10*, 433-436.
38. Kleiner, M.B., D.; Pelli, D.; Ingling, A.; Murray, R.; Broussard, C. What's new in psychtoolbox-3. *Perception* **2007**, *36*, 1-16.
39. Pelli, D.G. The VideoToolbox software for visual psychophysics: transforming numbers into movies. *Spat Vis* **1997**, *10*, 437-442.
40. Pavan, A.; Hobaek, M.; Blurton, S.P.; Contillo, A.; Ghin, F.; Greenlee, M.W. Visual short-term memory for coherent motion in video game players: evidence from a memory-masking paradigm. *Sci Rep* **2019**, *9*, 6027, doi:10.1038/s41598-019-42593-0.
41. Morgan, M.J.; Ward, R. Conditions for motion flow in dynamic visual noise. *Vision Res* **1980**, *20*, 431-435, doi:10.1016/0042-6989(80)90033-4.
42. Newsome, W.T.; Pare, E.B. A selective impairment of motion perception following lesions of the middle temporal visual area (MT). *J Neurosci* **1988**, *8*, 2201-2211.
43. Pavan, A.; Boyce, M.; Ghin, F. Action Video Games Improve Direction Discrimination of Parafoveal Translational Global Motion but Not Reaction Times. *Perception* **2016**, *45*, 1193-1202, doi:10.1177/0301006616663215.
44. Antal, A.; Kincses, T.Z.; Nitsche, M.A.; Paulus, W. Modulation of moving phosphene thresholds by transcranial direct current stimulation of V1 in human. *Neuropsychologia* **2003**, *41*, 1802-1807, doi:10.1016/s0028-3932(03)00181-7.
45. Stewart, L.; Battelli, L.; Walsh, V.; Cowey, A. Motion perception and perceptual learning studied by magnetic stimulation. *Electroencephalogr Clin Neurophysiol Suppl* **1999**, *51*, 334-350.
46. Cowey, A.; Campana, G.; Walsh, V.; Vaina, L.M. The role of human extra-striate visual areas V5/MT and V2/V3 in the perception of the direction of global motion: a transcranial magnetic stimulation study. *Exp Brain Res* **2006**, *171*, 558-562, doi:10.1007/s00221-006-0479-6.
47. Campana, G.; Maniglia, M.; Pavan, A. Common (and multiple) neural substrates for static and dynamic motion after-effects: a rTMS investigation. *Cortex* **2013**, *49*, 2590-2594, doi:10.1016/j.cortex.2013.07.001.
48. Laycock, R.; Crewther, D.P.; Fitzgerald, P.B.; Crewther, S.G. Evidence for fast signals and later processing in human V1/V2 and V5/MT+: A TMS study of motion perception. *J Neurophysiol* **2007**, *98*, 1253-1262, doi:10.1152/jn.00416.2007.
49. Pascual-Leone, A.; Bartres-Faz, D.; Keenan, J.P. Transcranial magnetic stimulation: studying the brain-behaviour relationship by induction of 'virtual lesions'. *Philos Trans R Soc Lond B Biol Sci* **1999**, *354*, 1229-1238, doi:10.1098/rstb.1999.0476.

50. Pascual-Leone, A.; Tarazona, F.; Keenan, J.; Tormos, J.M.; Hamilton, R.; Catala, M.D. Transcranial magnetic stimulation and neuroplasticity. *Neuropsychologia* **1999**, *37*, 207-217, doi:10.1016/s0028-3932(98)00095-5.
51. Pavan, A.; Alexander, I.; Campana, G.; Cowey, A. Detection of first- and second-order coherent motion in blindsight. *Exp Brain Res* **2011**, *214*, 261-271, doi:10.1007/s00221-011-2828-3.
52. Pavan, A.; Ghin, F.; Donato, R.; Campana, G.; Mather, G. The neural basis of form and form-motion integration from static and dynamic translational Glass patterns: A rTMS investigation. *Neuroimage* **2017**, *157*, 555-560, doi:10.1016/j.neuroimage.2017.06.036.
53. Schenk, T.; Ellison, A.; Rice, N.; Milner, A.D. The role of V5/MT+ in the control of catching movements: an rTMS study. *Neuropsychologia* **2005**, *43*, 189-198, doi:10.1016/j.neuropsychologia.2004.11.006.
54. Silvanto, J.; Cowey, A.; Lavie, N.; Walsh, V. Striate cortex (V1) activity gates awareness of motion. *Nat Neurosci* **2005**, *8*, 143-144, doi:10.1038/nn1379.
55. Walsh, V.; Ellison, A.; Battelli, L.; Cowey, A. Task-specific impairments and enhancements induced by magnetic stimulation of human visual area V5. *Proc Biol Sci* **1998**, *265*, 537-543, doi:10.1098/rspb.1998.0328.
56. Thompson, B.; Aaen-Stockdale, C.; Koski, L.; Hess, R.F. A double dissociation between striate and extrastriate visual cortex for pattern motion perception revealed using rTMS. *Hum Brain Mapp* **2009**, *30*, 3115-3126, doi:10.1002/hbm.20736.
57. Abrahamyan, A.; Clifford, C.W.; Ruzzoli, M.; Phillips, D.; Arabzadeh, E.; Harris, J.A. Accurate and rapid estimation of phosphene thresholds (REPT). *PLoS One* **2011**, *6*, e22342, doi:10.1371/journal.pone.0022342.
58. van de Ven, V.; Jacobs, C.; Sack, A.T. Topographic contribution of early visual cortex to short-term memory consolidation: a transcranial magnetic stimulation study. *J Neurosci* **2012**, *32*, 4-11, doi:10.1523/JNEUROSCI.3261-11.2012.
59. Pollack, I.N., D. A. A non-parametric analysis of recognition experiments. *Psychonomic Science* **1964**, *1*, 125-126.
60. Smith, W.D. Clarification of Sensitivity Measure A'. *Journal of Mathematical Psychology* **1995**, *39*, 82-89.
61. Zhang, J.M., Mueller, S.T. A note on ROC analysis and non-parametric estimate of sensitivity. *Psychometrika* **2005**, *70*, 203-212.
62. Green, D.M.S., J. A. *Signal detection theory and psychophysics*; 1966.
63. Stanislaw, H.; Todorov, N. Calculation of signal detection theory measures. *Behav Res Methods Instrum Comput* **1999**, *31*, 137-149, doi:10.3758/bf03207704.
64. Bates, D.M., M.; Bolker, B.; Walker, S.;. Fitting Linear Mixed-Effects Models Using lme4. *Journal of Statistical Software* **2015**, *67*, 1 - 48, doi:doi: 10.18637/jss.v067.i01.
65. Zuur, A.F.I., E. N.; Elphick, C. S. A protocol for data exploration to avoid common statistical problems. *Methods in Ecology and Evolution* **2010**, *1*, 3-14.
66. Zuur, A.F.I., E. N. A protocol for conducting and presenting results of regression-type analyses. *Methods in Ecology and Evolution* **2016**, *7*, 636-645.
67. Leys, C.L., C.; Klein, O.; Bernard, P.; Licata, L. Detecting outliers: Do not use standard deviation around the mean, use absolute deviation around the median. *Journal of Experimental Social Psychology* **2013**, *49*, 764-766.
68. Rousseeuw, P.J.C., C. Alternatives to the median absolute deviation. *Journal of the American Statistical Association* **1993**, *88*, 1273-1283.

69. Lo, S.; Andrews, S. To transform or not to transform: using generalized linear mixed models to analyse reaction time data. *Front Psychol* **2015**, *6*, 1171, doi:10.3389/fpsyg.2015.01171.
70. Deese, J.; Kaufman, R.A. Serial effects in recall of unorganized and sequentially organized verbal material. *J Exp Psychol* **1957**, *54*, 180-187, doi:10.1037/h0040536.
71. Murdock, B.B. The serial position effect of free recall. *Journal of Experimental Psychology* **1962**, *64*, 482-488.
72. Fougnie, D.; Suchow, J.W.; Alvarez, G.A. Variability in the quality of visual working memory. *Nat Commun* **2012**, *3*, 1229, doi:10.1038/ncomms2237.
73. van den Berg, R.; Awh, E.; Ma, W.J. Factorial comparison of working memory models. *Psychol Rev* **2014**, *121*, 124-149, doi:10.1037/a0035234.
74. Berens, P. CircStat: A Matlab Toolbox for Circular Statistics. *Journal of Statistical Software* **2009**, *31*, doi:http://www.jstatsoft.org/v31/i10.
75. Zar, J.H. *Biostatistical Analysis*; Prentice Hall, 1996.
76. Goris, R.L.; Movshon, J.A.; Simoncelli, E.P. Partitioning neuronal variability. *Nat Neurosci* **2014**, *17*, 858-865, doi:10.1038/nn.3711.
77. Cohen, M.R.; Maunsell, J.H. Attention improves performance primarily by reducing interneuronal correlations. *Nat Neurosci* **2009**, *12*, 1594-1600, doi:10.1038/nn.2439.
78. Cohen, M.R.; Maunsell, J.H. A neuronal population measure of attention predicts behavioral performance on individual trials. *J Neurosci* **2010**, *30*, 15241-15253, doi:10.1523/JNEUROSCI.2171-10.2010.
79. Suchow, J.W.; Brady, T.F.; Fougnie, D.; Alvarez, G.A. Modeling visual working memory with the MemToolbox. *J Vis* **2013**, *13*, doi:10.1167/13.10.9.
80. Wobbrock, J.O.F., L.; Gergle, D.; Higgins, J. J. The Aligned Rank Transform for nonparametric factorial analyses using only ANOVA procedures. In Proceedings of the Conference on Human Factors in Computing Systems, 2011; pp. 143-146.
81. Bates, D.M., M.; Bolker, B.; Walker, S. Fitting Linear Mixed-Effects Models Using lme4. *Journal of Statistical Software* **2015**, *67*, 1-48.
82. Cohen, D.; Goddard, E.; Mullen, K.T. Reevaluating hMT+ and hV4 functional specialization for motion and static contrast using fMRI-guided repetitive transcranial magnetic stimulation. *J Vis* **2019**, *19*, 11, doi:10.1167/19.3.11.
83. Maunsell, J.H.; van Essen, D.C. The connections of the middle temporal visual area (MT) and their relationship to a cortical hierarchy in the macaque monkey. *J Neurosci* **1983**, *3*, 2563-2586.
84. Maunsell, J.H.; Van Essen, D.C. Functional properties of neurons in middle temporal visual area of the macaque monkey. II. Binocular interactions and sensitivity to binocular disparity. *J Neurophysiol* **1983**, *49*, 1148-1167, doi:10.1152/jn.1983.49.5.1148.
85. Maunsell, J.H.; Van Essen, D.C. Functional properties of neurons in middle temporal visual area of the macaque monkey. I. Selectivity for stimulus direction, speed, and orientation. *J Neurophysiol* **1983**, *49*, 1127-1147, doi:10.1152/jn.1983.49.5.1127.
86. Born, R.T.; Bradley, D.C. Structure and function of visual area MT. *Annu Rev Neurosci* **2005**, *28*, 157-189, doi:10.1146/annurev.neuro.26.041002.131052.
87. Rust, N.C.M., V.; Simoncelli, E. P.; Movshon, J. A.;. How MT cells analyze the motion of visual patterns. *Nature neuroscience* **2006**, *9*, 1421 – 1431, doi:https://doi.org/10.1038/nn1786.

88. Galeano Weber, E.M.; Peters, B.; Hahn, T.; Bledowski, C.; Fiebach, C.J. Superior Intraparietal Sulcus Controls the Variability of Visual Working Memory Precision. *J Neurosci* **2016**, *36*, 5623-5635, doi:10.1523/JNEUROSCI.1596-15.2016.
89. Zhao, Y.; Kuai, S.; Zanto, T.P.; Ku, Y. Neural Correlates Underlying the Precision of Visual Working Memory. *Neuroscience* **2020**, *425*, 301-311, doi:10.1016/j.neuroscience.2019.11.037.
90. Zokaei, N.; Manohar, S.; Husain, M.; Feredoes, E. Causal evidence for a privileged working memory state in early visual cortex. *J Neurosci* **2014**, *34*, 158-162, doi:10.1523/JNEUROSCI.2899-13.2014.
91. Rademaker, R.L.; van de Ven, V.G.; Tong, F.; Sack, A.T. The impact of early visual cortex transcranial magnetic stimulation on visual working memory precision and guess rate. *PLoS One* **2017**, *12*, e0175230, doi:10.1371/journal.pone.0175230.
92. Zhang, W.; Luck, S.J. Discrete fixed-resolution representations in visual working memory. *Nature* **2008**, *453*, 233-235, doi:10.1038/nature06860.
93. Pertzov, Y.; Bays, P.M.; Joseph, S.; Husain, M. Rapid forgetting prevented by retrospective attention cues. *J Exp Psychol Hum Percept Perform* **2013**, *39*, 1224-1231, doi:10.1037/a0030947.